

An improved calculation of the isospin-symmetry-breaking corrections to Superaligned Fermi β decay

I.S. Towner* and J.C. Hardy

Cyclotron Institute, Texas A & M University, College Station, Texas 77843

(Dated: February 2, 2008)

We report new shell-model calculations of the isospin-symmetry-breaking correction, δ_C , to superallowed $0^+ \rightarrow 0^+$ nuclear β decay. The most important improvement is the inclusion of core orbitals, which are demonstrated to have a significant impact on the mismatch in the radial wave functions of the parent and daughter states. We determine which core orbitals are important to include from an examination of measured spectroscopic factors in single-nucleon pick-up reactions. In addition, where new sets of effective interactions have become available since our last calculation, we now include them; this leads to small changes in δ_{NS} as well. We also examine the new radiative-correction calculation by Marciano and Sirlin and, by a simple reorganization, show that it is possible to preserve the conventional separation into a nucleus-independent “inner” radiative term, Δ_R^V , and a nucleus-dependent “outer” term, δ_R' . We tabulate the new values for δ_C , δ_{NS} and δ_R' for twenty superallowed transitions, including the thirteen currently well-studied cases. With these new correction terms the corrected $\mathcal{F}t$ values for the thirteen cases are statistically consistent with one another and the anomalousness of the ^{46}V result disappears. These new calculations lead to a lower average $\overline{\mathcal{F}t}$ value and a higher value for V_{ud} . The sum of squares of the top-row elements of the CKM matrix now agrees exactly with unitarity.

PACS numbers: 23.40.Bw, 23.40.Hc

I. INTRODUCTION

Superaligned $0^+ \rightarrow 0^+$ nuclear β decay currently provides the most precise value for V_{ud} , the up-down element of the Cabibbo-Kobayashi-Maskawa (CKM) matrix [1, 2, 3]. This element is the key ingredient of the most demanding available test of CKM-matrix unitarity, a fundamental requirement of the electroweak standard model. To extract V_{ud} from the experimental data, small theoretical corrections – of order $\sim 1\%$ – must be applied to take account of unobserved radiative effects as well as the isospin symmetry-breaking that occurs between the analog parent and daughter states of each superallowed transition [4, 5]. Even though these corrections are very small, experimental measurements have by now reached such high precision that the uncertainty on V_{ud} ($\pm 0.03\%$) is currently dominated not by experiment but by the uncertainty on these theoretical corrections.

In the determination of V_{ud} , an important strength of the nuclear measurements is that there are many $0^+ \rightarrow 0^+$ transitions available for study, and currently there are thirteen of them, ranging from ^{10}C to ^{74}Rb , that have been measured with high precision. With so many, it becomes possible to validate the analysis procedure by checking that all transitions individually yield statistically consistent results for V_{ud} . Since the isospin-symmetry-breaking corrections depend on nuclear structure, they differ from transition to transition and are particularly sensitive to this consistency test. Thus the

appearance of an anomalous result from any transition could signal a problem with the structure-dependent correction for that case, a problem which might have implications for other cases as well.

In the most recent survey of superallowed $0^+ \rightarrow 0^+$ transitions, which appeared in 2005 [1], the results for all precisely measured cases – there were twelve at that time – were statistically consistent with one another. Today, there are thirteen such cases and they still form a statistically consistent ensemble overall. However, recent precise Penning-trap measurements [6, 7] of the Q_{EC} value for the superallowed decay of ^{46}V have left the result for that transition more than two standard deviations away from the average of all other well-known transitions. This possible anomaly led us initially to re-examine the isospin-symmetry-breaking corrections for the ^{46}V transition, but what we learned from that re-examination prompted us to a more general reevaluation of the corrections for other transitions as well.

Our previous shell-model calculations for ^{46}V considered six valence nucleons occupying the pf -shell orbitals outside a ^{40}Ca closed shell. This model space generated reasonable energies and spins for the known states in ^{46}Ti , the daughter of ^{46}V . However, an important part of the charge-dependent correction depends on the radial mismatch between the decaying proton in the parent nucleus and the resulting neutron in the daughter nucleus; but both these nucleons are bound to ^{45}Ti , so the structure of that nucleus turns out to be important too. What is most striking about ^{45}Ti is that it has a $3/2^+$ state at an excitation energy of only 330 keV, which is strongly populated in single-nucleon pick-up reactions like (p, d) and $(^3\text{He}, \alpha)$. Such low-lying sd -shell states can contribute to the structural parentage of the

*Present address: Department of Physics, Queen's University, Kingston, Ontario K7L 3N6, Canada

initial and final states of the superallowed transition and consequently must affect the radial mismatch between them. This indicated to us that a complete calculation of the isospin-symmetry-breaking correction for the decay of ^{46}V should include contributions from shells deeper than the pf shell.

Two questions then arose. How many deeper shells need to be included and, if this effect is important for ^{46}V decay, how many other transitions will be similarly affected? In section III of this paper, we address these questions and settle on criteria for including deeper shells. Using these criteria – and incorporating more recent effective interactions that have become available since our last work – we then re-evaluate the isospin-symmetry-breaking corrections for all transitions of relevance to the study of superallowed $0^+ \rightarrow 0^+\beta$ decay. For the cases with $A \leq 38$ the changes in the corrections are very small – typically 0.03% – but for the heavier nuclei the changes can be as large as 0.2%. Most significantly, with the new calculated corrections, the result for ^{46}V is no longer anomalous.

In section IV, we incorporate recent improvements made by Marciano and Sirlin [8] to the calculation of the radiative corrections for superallowed decays and then in section V we apply both types of corrections – isospin-symmetry-breaking and radiative – to the current experimental data for superallowed decays. The result for V_{ud} is changed appreciably, although it is still within quoted uncertainties of its old value, and the CKM-unitarity sum is improved.

II. SUPERALLOWED BETA DECAY

Superallowed Fermi beta decay between 0^+ states depends uniquely on the vector part of the hadronic weak interaction. When it occurs between isospin $T = 1$ analog states, the conserved vector current (CVC) hypothesis indicates that the ft values should be the same irrespective of the nucleus, *viz.*

$$ft = \frac{K}{G_V^2 |M_F|^2} = \text{const}, \quad (1)$$

where $K/(\hbar c)^6 = 2\pi^3 \hbar \ln 2 / (m_e c^2)^5 = (8120.278 \pm 0.004) \times 10^{-10} \text{ GeV}^{-4}\text{s}$; G_V is the vector coupling constant for semi-leptonic weak interactions; and M_F is the Fermi matrix element. The CVC hypothesis asserts that the vector coupling constant, G_V , is a true constant and not renormalised to another value in the nuclear medium.

In practice, Eq. (1) has to be amended slightly. Firstly, there are radiative corrections because, for example, the emitted electron may emit a bremsstrahlung photon that goes undetected in the experiment. Secondly, isospin is not an exact symmetry in nuclei so the nuclear matrix element, M_F , is slightly reduced from its ideal value, leading us to write:

$$|M_F|^2 = |M_0|^2 (1 - \delta_C), \quad (2)$$

where M_0 is the exact-symmetry value, which for $T = 1$ states is $M_0 = \sqrt{2}$. Thus, we define a “corrected” $\mathcal{F}t$ value as

$$\mathcal{F}t \equiv ft(1 + \delta_R)(1 - \delta_C) = \frac{K}{2G_V^2(1 + \Delta_R^V)} = \text{const}, \quad (3)$$

where δ_C is the isospin-symmetry-breaking correction, δ_R is the transition-dependent part of the radiative correction, and Δ_R^V is the transition-independent part. Fortunately these corrections are all of order 1% but, even so, to maintain an accuracy criterion of 0.1% they must be calculated with an accuracy of 10% of their central value. This is a demanding request, especially for the nuclear-structure-dependent corrections.

To separate out those terms that are dependent on nuclear structure from those that are not, we split the transition-dependent radiative correction into two terms,

$$\delta_R = \delta'_R + \delta_{NS}, \quad (4)$$

of which the first, δ'_R , is a function only of the electron’s energy and the charge of the daughter nucleus Z ; it therefore depends on the particular nuclear decay, but is *independent* of nuclear structure. The second term, δ_{NS} , like δ_C , depends in its evaluation on the details of nuclear structure. To emphasize the different sensitivities of the correction terms, we rewrite the expression for $\mathcal{F}t$ as

$$\mathcal{F}t \equiv ft(1 + \delta'_R)(1 + \delta_{NS} - \delta_C) = \frac{K}{2G_V^2(1 + \Delta_R^V)}, \quad (5)$$

where the first correction in brackets is independent of nuclear structure, while the second incorporates the structure-dependent terms.

From Eq. (5) it can be seen that a measurement of any one superallowed transition establishes a single value for G_V ; moreover, measurements of many transitions provides an excellent test of the validity of the whole analysis. Since CVC requires a unique value of G_V , all the extracted $\mathcal{F}t$ -values should be identical within experimental uncertainties.

The ft -value that characterizes any β -transition depends on three measured quantities: the total transition energy, Q_{EC} ; the half-life, $t_{1/2}$, of the parent state; and the branching ratio, R , for the particular transition of interest. The Q_{EC} -value is required to determine the statistical rate function, f , while the half-life and branching ratio combine to yield the partial half-life, t . In 2005 we published a new survey of world data on superallowed $0^+ \rightarrow 0^+$ beta decays [1]. All previously published measurements were included, even those that were based on outdated calibrations if enough information was provided that they could be corrected to modern standards. In all, more than 125 independent measurements of comparable precision, spanning four decades, made the cut. In the two years since the survey was closed another ten relevant publications have appeared [6, 7, 9, 10, 11, 12, 13, 14, 15, 16] and we have now incorporated these results into our data base. Based on these

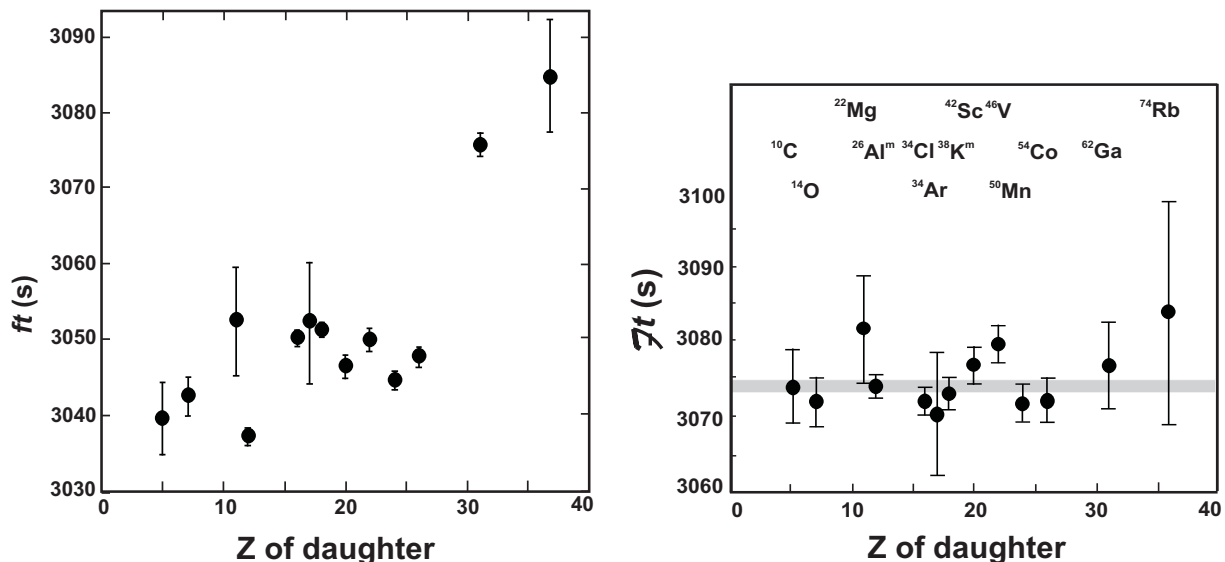


FIG. 1: Results from the 2005 survey [1] updated with more recent published results [6, 7, 9, 10, 11, 12, 13, 14, 15, 16]. The uncorrected ft values for the thirteen best known superallowed decays (left) are compared with the same results after corrections have been applied to obtain Ft values. Here we have used the corrections calculated by us in 2002 [4], which were used in the original survey. The shaded horizontal band gives one standard deviation around the average Ft value.

data for the thirteen most precisely known transitions, we obtain the ft values shown on the left side of Figure 1; then, by incorporating the corrections calculated by us in 2002 [4] and used in our 2005 survey [1], we obtain the corrected Ft values plotted on the right side of the figure.

Obviously the calculated corrections do a remarkable job eliminating the considerable scatter that is evident in the ft -value plot on the left but is absent in the corrected Ft values shown on the right. Overall, the statistical agreement among the Ft values is quite satisfactory, the normalized χ^2 being 0.8. Thus, considering that the correction terms were evaluated completely independently of these data, the consistency among the Ft values can be taken as strong evidence that the correction terms are, in general, soundly based.

However, there is a small but noticeable deviation from the average at ^{46}V (and possibly ^{42}Sc), which has only been revealed by the recent Penning-trap measurements [6, 7] of the transition Q_{EC} values. Though its statistical significance appears rather marginal in the figure, it must be remarked that the uncertainties quoted on these Ft values have been very conservatively determined. The measured data for each input parameter – Q_{EC} -value, half-life and branching ratio – were separately evaluated [1] and, if the measurements were inconsistent with one another, the weighted-average uncertainty for that parameter was increased to account for that inconsistency. In effect, for such cases, the original uncertainties quoted with the published measurements were all increased by a common “scale factor” that was large enough to restore statistical consistency among the measurements. (These scale factors are tabulated for each parameter in Ref. [1];

they range from 1 to 3.6.) This method, which is also used by the Particle Data Group [17], leads to final average values that have a high confidence level but it does so at the cost of producing uncertainties that are in many cases larger than would result from a strict statistical average.

With this method of analysis in mind, the excursion of the ^{46}V Ft value cannot be entirely ignored as a possible signal that the nuclear-structure-dependent corrections in this mass region are deficient. It certainly proved to be sufficiently provocative that we were led to the reevaluation of correction terms that is reported here.

III. ISOSPIN-SYMMETRY BREAKING CORRECTION, δ_C

For weak vector interactions in hadron states, the CVC hypothesis protects the decay amplitudes from strong-interaction corrections. However, there is a caveat. The CVC hypothesis also requires the hadron state to be an exact eigenstate of $SU(2)$ symmetry (isospin). In nuclei, $SU(2)$ is always broken, albeit weakly, by Coulomb interactions between protons. There may be other charge-dependent effects as well. These influences shift the value of the hadron matrix element from its exact symmetry limit to a new value and this shift has to be evaluated before weak-interaction physics can be probed with hadrons. In the case of superallowed β decay, the hadron matrix element, M_F , is given by Eq. (2) and it is δ_C that we seek to evaluate.

In the shell model for the cases of interest here, the A -particle wave functions representing the initial and final

states for superallowed β decay, $|i\rangle$ and $|f\rangle$, are states of angular momentum zero and isospin one. In a second quantisation formulation, the Fermi matrix element is written

$$M_F = \langle f | \tau_+ | i \rangle = \sum_{\alpha, \beta} \langle f | a_\alpha^\dagger a_\beta | i \rangle \langle \alpha | \tau_+ | \beta \rangle, \quad (6)$$

where the operator for Fermi β decay is the isospin ladder operator, a_α^\dagger creates a neutron in quantum state α and a_β annihilates a proton in quantum state β . The single-particle matrix element, $\langle \alpha | \tau_+ | \beta \rangle$, is just a radial integral

$$\langle \alpha | \tau_+ | \beta \rangle = \delta_{\alpha, \beta} \int_0^\infty R_\alpha^n(r) R_\beta^p(r) r^2 dr \equiv \delta_{\alpha, \beta} r_\alpha. \quad (7)$$

If the proton and neutron radial functions $R_\alpha^n(r)$ and $R_\beta^p(r)$ are identical, then the radial integral reduces to the normalization integral and has the value $r_\alpha = 1$.

Now we introduce into Eq. (6) a complete set of states for the $(A-1)$ -particle system, $|\pi\rangle$, by writing

$$M_F = \sum_{\pi, \alpha} \langle f | a_\alpha^\dagger | \pi \rangle \langle \pi | a_\alpha | i \rangle r_\alpha^\pi. \quad (8)$$

This is the essence of our model: we have allowed the radial integral to depend on the parentage expansion. Thus, we have added an additional label to r_α and now write r_α^π .

If isospin is an exact symmetry, then the matrix elements of the creation and annihilation operators are related by hermiticity, $\langle \pi | a_\alpha | i \rangle = \langle f | a_\alpha^\dagger | \pi \rangle^*$. With that requirement, and with the radial integrals set to unity, the symmetry-limit matrix element is

$$M_0 = \sum_{\pi, \alpha} |\langle f | a_\alpha^\dagger | \pi \rangle|^2. \quad (9)$$

Thus we see that the breakdown of isospin symmetry can enter the evaluation of M_F in one of two ways: either the matrix elements of a_α and a_α^\dagger are not related by hermiticity, or the radial integrals are not unity. Since each effect is small, we can, to first order, write the isospin-symmetry breaking correction as the sum of two terms

$$\delta_C = \delta_{C1} + \delta_{C2} \quad (10)$$

where in evaluating δ_{C1} all radial integrals are set to unity but the matrix elements are not assumed to be related by hermiticity, while in evaluating δ_{C2} it is assumed that $\langle \pi | a_\alpha | i \rangle = \langle f | a_\alpha^\dagger | \pi \rangle^*$ but the radial integrals are allowed to differ from unity. Past calculations [4, 5] have indicated the radial overlap correction, δ_{C2} , is the larger of the two corrections so we will study this first.

A. Radial Overlap Correction, δ_{C2}

1. Strategy for calculation

For the δ_{C2} calculation, the Fermi matrix element is

$$M_F = \sum_{\pi, \alpha} |\langle f | a_\alpha^\dagger | \pi \rangle|^2 r_\alpha^\pi$$

$$\begin{aligned} &= \sum_{\pi, \alpha} |\langle f | a_\alpha^\dagger | \pi \rangle|^2 - \sum_{\pi, \alpha} |\langle f | a_\alpha^\dagger | \pi \rangle|^2 (1 - r_\alpha^\pi) \\ &= M_0 \left(1 - \frac{1}{M_0} \sum_{\pi, \alpha} |\langle f | a_\alpha^\dagger | \pi \rangle|^2 \Omega_\alpha^\pi \right) \end{aligned} \quad (11)$$

where M_0 is the exact-symmetry value, Eq. (9), and Ω_α^π has been introduced as a radial-mismatch factor

$$\Omega_\alpha^\pi = (1 - r_\alpha^\pi). \quad (12)$$

Recalling that δ_{C2} is defined as $|M_F|^2 = |M_0|^2 (1 - \delta_{C2})$ we obtain

$$\delta_{C2} \simeq \frac{2}{M_0} \sum_{\pi, \alpha} |\langle f | a_\alpha^\dagger | \pi \rangle|^2 \Omega_\alpha^\pi \quad (13)$$

to first order in small quantities. A large contribution to δ_{C2} therefore requires a large spectroscopic amplitude and a significant departure of the radial integral from unity.

There is an opportunity here to take guidance from experiment. The square of each spectroscopic amplitude, $|\langle f | a_\alpha^\dagger | \pi \rangle|^2$, is related to the spectroscopic factor measured in neutron pick-up direct reactions. The exact relation, after inserting the isospin angular momentum couplings, is

$$\delta_{C2} \simeq \sum_{\pi, \alpha} \frac{T_f(T_f + 1) + \frac{3}{4} - T_\pi(T_\pi + 1)}{T_f(T_f + 1)} S_{\alpha, T_f}^{T_\pi} \Omega_\alpha^\pi \quad (14)$$

where $S_{\alpha, T_f}^{T_\pi}$ is the spectroscopic factor for pick up of a neutron in quantum state α from an A -particle state of isospin T_f to an $(A-1)$ -particle state of isospin T_π . On setting $T_f = 1$ and separately identifying sums to the isospin-lesser states with $T_\pi = \frac{1}{2}$, denoted $\pi^<$, and the isospin-greater states with $T_\pi = \frac{3}{2}$, denoted $\pi^>$, we obtain a very revealing formula

$$\delta_{C2} \simeq \sum_{\pi^<, \alpha} S_\alpha^< \Omega_\alpha^< - \frac{1}{2} \sum_{\pi^>, \alpha} S_\alpha^> \Omega_\alpha^>. \quad (15)$$

This equation provides the key to the strategy we will use in calculating δ_{C2} . It demonstrates that there is a cancellation between the contributions of the isospin-lesser states and the isospin-greater states. Moreover, if the orbital α were completely full in the initial A -particle wavefunction, then the Macfarlane and French sum rules [19] for spectroscopic factors would require $\sum_{\pi^<} S_\alpha^< = \frac{1}{2} \sum_{\pi^>} S_\alpha^>$ and the cancellation in Eq. (15) would be very strong. In fact, the cancellation would be complete if $\Omega_\alpha^< = \Omega_\alpha^>$. As we will discuss further in the next section, this cancellation is not in general complete because the radial-mismatch factors for isospin-lesser states are larger than those for isospin-greater states. Even so, cancellation is always significant, and it becomes most complete when closed-shell orbitals are involved. Furthermore, the more deeply bound the closed-shell orbital, the greater the energy spread in the spectroscopic strength and the

TABLE I: Illustration of the strategy used in calculating δ_{C2} for ^{46}V . The measured spectroscopic factors from the $^{46}\text{Ti}(^3\text{He}, \alpha)^{45}\text{Ti}$ reaction [18] are shown for the states where they are largest. Two calculations are then given for each state's contribution to δ_{C2} : the first assumes that the total Macfarlane-French (M-F) sum rule is exhausted in each state, while the second gives the result of a complete shell-model calculation. Both methods give remarkably similar results.

^{45}Ti $E_x(\text{keV})$	$J^\pi; T_\pi$	α	$(^3\text{He}, \alpha)$ measured [18]		Limiting case		Shell Model	
			S_α	$\Omega_\alpha(\%)$	M-F sum rule	contribution to $\delta_{C2}(\%)$	$\sum_\pi S_\alpha^\pi$	contribution to $\delta_{C2}(\%)$
0	$\frac{7}{2}^-, \frac{1}{2}$	$f_{7/2}$	2.7(11)	0.134	3.33	0.45	3.36	0.45
330	$\frac{3}{2}^+, \frac{1}{2}$	$d_{3/2}$	1.9(8)	0.157	2.67	0.42	2.45	0.39
1566	$\frac{1}{2}^+, \frac{1}{2}$	$s_{1/2}$	0.7(3)	0.318	1.33	0.42	1.22	0.39
4723	$\frac{7}{2}^-, \frac{3}{2}$	$f_{7/2}$	3.6(16)	0.085	2.67	-0.11	2.74	-0.12
4810	$\frac{3}{2}^+, \frac{3}{2}$	$d_{3/2}$	3.6(16)	0.100	5.33	-0.27	4.92	-0.25
5760	$\frac{1}{2}^+, \frac{3}{2}$	$s_{1/2}$	3.2(12)	0.224	2.67	-0.30	2.47	-0.28

more complete the cancellation. Thus, although the dominant contributions to δ_{C2} come from unfilled orbitals, we conclude that closed-shell orbitals must play a role, albeit one that decreases in importance as the orbitals become more deeply bound.

Based on these observations, our strategy is to use experiment to guide us in determining which closed-shell orbitals are important enough to include. Ideally, of course, one would take the spectroscopic factors determined from experiment and insert them into Eq. (15) but, especially where delicate cancellations are involved, the reliability of (forty-year-old) experimental spectroscopic factors is certainly not up to the task. Our strategy then is to use the shell model to calculate the spectroscopic amplitudes in Eq. (13) but to limit the sum over orbitals α just to those for which large spectroscopic factors have been observed in neutron pick-up reactions.

We illustrate the strategy for the case of ^{46}V . The spectroscopic factors for neutron pick up from ^{46}Ti have been measured in the $(^3\text{He}, \alpha)$ reaction by Borlin [18]. He identified sixteen states in ^{45}Ti , and in Table I we record the six states with the largest spectroscopic factors, *i.e.* $S > 0.5$. We note that the errors on the experimental spectroscopic factors are quite large, and in two cases the quoted S_α values (column 4) exceed the Macfarlane-French sum rule [19] for pure configurations (column 6). Thus we do not use the experimental spectroscopic factor explicitly, but take them as a guide for which orbitals should be included in the shell-model calculation. In the case of ^{46}V decay, they tell us that orbitals $f_{7/2}$, $d_{3/2}$ and $s_{1/2}$ should be included. In column five of Table I we give a typical value for the radial mismatch factor, Ω_α^π , for the given orbital α and isospin T_π . Column seven gives the contribution to δ_{C2} from this α and isospin T_π if the Macfarlane-French sum rule is used for the spectroscopic factor, while in columns eight and nine are shown the results of a detailed shell-model calculation. The results from the Macfarlane-French sum rules and the shell-

model calculation are remarkably similar. The summed δ_{C2} for the shell-model calculation (the sum of all entries in column 9) is 0.58%, nearly a factor of two larger than our previous calculated value, which was published in 2002 [4].

The difference between our calculations arises as follows: In 2002 our shell-model calculations for ^{46}V were based on the model space $(fp)^6$, with six valence nucleons occupying the pf -shell orbitals. In fact, only the $f_{7/2}$ orbital contributed importantly to the δ_{C2} calculation so the result was $\delta_{C2} = 0.45 - 0.12 = 0.33\%$ (see the two rows for the $f_{7/2}$ orbital in Table I). Absent from this 2002 calculation was any contribution from the core orbitals, $d_{3/2}$ and $s_{1/2}$. In our present calculations, these orbitals are included, with the $d_{3/2}$ orbital contributing 0.14 % to δ_{C2} and the $s_{1/2}$ contributing 0.11 %.

But why stop there? Why not include the $d_{5/2}$ and possibly the p -shell orbitals in the computation? Our answer is that the neutron pick-up measurement saw little or no evidence for such core states, which implies that their spectroscopic strength is distributed widely over many states. In this case, the cancellation between isospin-lesser and isospin-greater states becomes more complete and their contribution to δ_{C2} is reduced to a level that we believe can be neglected.

With this approach, we are now in a position to revise our earlier results [4] to include the effects of previously ignored core orbitals. Again using measured spectroscopic factors from neutron pick-up reactions, we determined that changes were required for the $A = 22$ and 26 cases, in which p -shell holes must contribute in addition to the original sd -shell configurations; similarly, sd -shell holes were required in addition to the pf -shell particles for $A = 46$, 50 and 54. For $A = 62$, 66, 70 and 74 in the upper pf -shell there are no experimental neutron pick-up reaction measurements to guide us. Our previously published calculations for these nuclei were based on $(p_{3/2}, f_{5/2}, p_{1/2})^n$ model spaces using ^{56}Ni as

a closed-shell core. It seemed prudent now for these cases at least to include the $f_{7/2}$ orbital in the calculation of δ_{C2} , and we have made this change. In the cases with $A = 18$ and 42 , we had previously included some contribution from deeper shells; we did not need to make any changes in the former but did add the $s_{1/2}$ and $d_{5/2}$ shells to the latter. No additional orbitals were required for the cases with $A = 10, 14, 30, 34$ and 38 .

2. Radial-mismatch Factor, Ω_α^π

In considering the radial integrals, we benefit from a very strong constraint: the asymptotic forms of all radial functions must match the measured separation energies, S_p and S_n , where S_p is the proton separation energy in the decaying nucleus and S_n the neutron separation energy in the daughter nucleus. The basic ingredients of these separation energies are well known and can be found in any atomic mass tables. It is the size of the difference between S_p and S_n and the presence or absence of nodes in the radial wave functions that are the principal factors in determining the magnitude of Ω_α^π .

Our calculations of this mismatch factor follows the same path as that described in our earlier works [4, 20]. We use a Saxon-Woods potential defined for a nucleus of mass A and charge $Z + 1$ as:

$$V(r) = -V_0 f(r) - V_s g(r) \mathbf{l} \cdot \boldsymbol{\sigma} + V_C(r) - V_g g(r) - V_h h(r), \quad (16)$$

where

$$\begin{aligned} f(r) &= \{1 + \exp((r - R)/a)\}^{-1}, \\ g(r) &= \left(\frac{\hbar}{m_\pi c}\right)^2 \frac{1}{a_s r} \exp\left(\frac{r - R_s}{a_s}\right) \\ &\quad \times \left\{1 + \exp\left(\frac{r - R_s}{a_s}\right)\right\}^{-2}, \\ h(r) &= a^2 \left(\frac{df}{dr}\right)^2, \\ V_C(r) &= Ze^2/r, \quad \text{for } r \geq R_c \\ &= \frac{Ze^2}{2R_c} \left(3 - \frac{r^2}{R_c^2}\right), \quad \text{for } r < R_c, \end{aligned} \quad (17)$$

with $R = r_0(A - 1)^{1/3}$ and $R_s = r_s(A - 1)^{1/3}$. The first three terms in Eq. (16) are the central, spin-orbit and Coulomb terms respectively. The fourth and fifth terms are additional surface terms whose role we discuss shortly.

Most of the parameters were fixed at standard values, $V_s = 7$ MeV, $r_s = 1.1$ fm and $a = a_s = 0.65$ fm. The radius of the Coulomb potential was determined from the charge mean square radius, $\langle r^2 \rangle_{\text{ch}}^{1/2}$, of the decaying nucleus as determined from elastic electron scattering; see Eqs. (21) and (22) in Ref. [4]. The well radius, r_0 , was similarly fixed, by requiring that the charge density constructed from the square of the proton wave functions

bound in the well should also match the charge mean square radius. Initially, with V_g and V_h set to zero, the well depth, V_0 , was adjusted so that the binding energy of the least-bound orbital matched the experimental separation energy.

From the shell model calculation, we obtained the A -particle wave functions, $|i\rangle$ and $|f\rangle$, expanded into products of $(A - 1)$ -particle wave functions $|\pi\rangle$ and single-particle functions $|\alpha\rangle$. In Eq. (8) and the discussion that followed it, we noted that the radial integral should depend on the separation energies relative to the $(A - 1)$ state, $|\pi\rangle$. We ultimately allowed this to happen but initially we calculated the value of δ_{C2} under the assumption that the proton and neutron radial functions, $R^p(r)$ and $R^n(r)$, have asymptotic forms for all α that are fixed at the separation energies, S_p and S_n , to the ground state of the $(A - 1)$ nucleus. In this case, the sums over π can be done analytically and the computed value of δ_{C2} becomes independent of the shell-model effective interaction. This result, which we label δ_{C2}^I , can be simply expressed with the help of Eqs. (9) and (13):

$$\delta_{C2}^I \simeq 2\Omega_{\alpha_g}. \quad (18)$$

Here α_g is the shell-model orbital of the transferred neutron in the pick-up reaction from the A -particle state $|f\rangle$ to the ground state of the $(A - 1)$ -particle nucleus.

We next removed our simplifying assumption and evaluated the radial integrals with eigenfunctions of the Saxon-Woods potential whose well depth was adjusted so that each eigenfunction matched the separation energy of the $(A - 1)$ state to which it corresponds, $|\pi\rangle$. For an $(A - 1)$ state at excitation energy E_x the corresponding separation energies are $S_p + E_x$ and $S_n + E_x$. We label these results δ_{C2}^{II} and note that the values now depend on the spectroscopic amplitudes, and hence on the shell-model effective interaction, but not strongly.

So far, we have ignored the two surface terms in Eq. (17) by setting $V_g = 0$ and $V_h = 0$. It can be argued, however, that the central part of the potential, which in principle should be determined from some Hartree-Fock procedure, should not be continually adjusted. Instead, any adjustments made to match separation energies should be to the surface part of the potential rather than to the depth of the well. Thus, we also calculated δ_{C2} by fixing V_0 separately for protons and neutrons to match the ground-state parent separation energies, S_p and S_n , and then adjusting the strength of the surface term, V_g (keeping $V_h = 0$) so that the asymptotic forms matched the separation energies $S_p + E_x$ and $S_n + E_x$. These results are labelled δ_{C2}^{III} .

Finally, our fourth method of calculation was the same as the third, except that it was the second surface term, V_h , that was adjusted to match separation energies, keeping $V_g = 0$. This second term, $h(r)$, is even more strongly peaked in the surface than $g(r)$. These results are labelled δ_{C2}^{IV} .

On average, the method III values of δ_{C2} are about 2% lower than the method II values; and method IV values

are about 7% lower than the method II values for orbitals without any radial nodes. For orbitals with one or more nodes, there is more of the radial wave function in the surface region and methods III and IV produce greater reductions.

3. The shell-model calculations

We now present our results for δ_{C2} based on the extensions of the shell-model spaces mentioned at the end of Sect. III A 1. In addition to adding the core orbitals mentioned there, however, in some cases we have also been able to make use of more recent effective interactions that have become available since our last work. Specifically, we have used the following interactions in the various mass regions of interest: In the p -shell, we use the Cohen-Kurath interactions [21] and the more recent PWB interaction of Warburton and Brown [22]. In the s, d -shell, besides the universal interaction of Wildenthal [23], we employ two new versions, USD-A and USD-B, of Brown and Richter [24]. In the pf -shell we use the KB3 interaction of Kuo-Brown [25] as modified by Poves and Zuker [26], the FPMI3 interaction of Richter and Brown [27], and the more recent GXPF1 interaction of Honma *et al.* [28, 29]. For cross-shell interactions between the major shells, we have used the interaction of Millener and Kurath [30]. It should be noted that in many cases we found it necessary to introduce some truncations in the original model space in order to keep the calculations tractable.

We made calculations for all twenty superallowed transitions considered in our earlier work [1, 4], and for each we calculated δ_{C2} in the four methods, I-IV, described in Sect. III A 2 and with the several interactions listed in the previous paragraph. In Table II we record only *one sample result* for δ_{C2}^I , δ_{C2}^{II} , δ_{C2}^{III} and δ_{C2}^{IV} for each nucleus listed. However, our “adopted δ_{C2} ” values result from our assessment of *all* multiple-parentage calculations made for each decay, not just those shown in the previous three columns. The uncertainty assigned to each adopted value reflects the uncertainty in the radius of the Saxon-Woods potential (resulting from an uncertainty in the nuclear rms radius to which it is adjusted), the spread of results obtained with different shell-model interactions, and the spread of results obtained with the different procedures labelled II, III and IV in the Table.

B. Isospin-Mixing Correction, δ_{C1}

The second (and smaller) contribution to δ_C is the isospin-mixing correction, δ_{C1} . For its evaluation, the radial integrals are all set to unity, but the spectroscopic amplitudes in Eq. (8) are not required to satisfy hermiticity. Calculations of this correction turn out to be very sensitive to the details of the shell-model computation. This would be a very unfortunate property if we were

TABLE II: Calculations of δ_{C2} with Saxon-Woods radial functions, without parentage expansions (δ_{C2}^I) and with parentage expansions (δ_{C2}^{II} , δ_{C2}^{III} , and δ_{C2}^{IV}). Note that only one sample result is shown in each case for δ_{C2}^I , δ_{C2}^{II} , δ_{C2}^{III} and δ_{C2}^{IV} , while the adopted δ_{C2} value in column 7 reflects the results from all multiple-parentage calculations for that case; see text.

2002		This work				
Parent nucleus	$\delta_{C2}(\%)$ Ref. [4]	$\delta_{C2}^I(\%)$	$\delta_{C2}^{II}(\%)$	$\delta_{C2}^{III}(\%)$	$\delta_{C2}^{IV}(\%)$	$\delta_{C2}(\%)$ adopted
$T_z = -1 :$						
^{10}C	0.170(15)	0.132	0.163	0.165	0.163	0.165(15)
^{14}O	0.270(15)	0.217	0.274	0.271	0.271	0.275(15)
^{18}Ne	0.390(10)	0.251	0.386	0.387	0.382	0.410(25)
^{22}Mg	0.255(10)	0.207	0.366	0.382	0.375	0.370(20)
^{26}Si	0.330(10)	0.223	0.421	0.407	0.392	0.405(25)
^{30}S	0.740(20)	0.812	0.714	0.710	0.713	0.700(20)
^{34}Ar	0.610(40)	0.351	0.680	0.639	0.579	0.635(55)
^{38}Ca	0.710(50)	0.402	0.840	0.784	0.702	0.745(70)
^{42}Ti	0.555(40)	0.359	0.881	0.849	0.780	0.835(75)
$T_z = 0 :$						
$^{26}\text{Al}^m$	0.230(10)	0.156	0.292	0.280	0.271	0.280(15)
^{34}Cl	0.530(30)	0.312	0.583	0.561	0.498	0.550(45)
$^{38}\text{K}^m$	0.520(40)	0.299	0.623	0.575	0.522	0.550(55)
^{42}Sc	0.430(30)	0.278	0.681	0.648	0.606	0.645(55)
^{46}V	0.330(25)	0.273	0.587	0.543	0.506	0.545(55)
^{50}Mn	0.450(30)	0.315	0.638	0.598	0.594	0.610(50)
^{54}Co	0.570(40)	0.376	0.760	0.688	0.706	0.720(60)
^{62}Ga	1.05(15)	1.31	1.22	1.19	1.14	1.20(20)
^{66}As	1.15(15)	1.32	1.41	1.34	1.24	1.35(40)
^{70}Br	1.00(20)	1.43	1.41	1.31	1.10	1.25(25)
^{74}Rb	1.30(40)	1.68	1.60	1.47	1.12	1.50(30)

not able to adopt certain strategies that act to reduce the model dependence considerably.

There are three ways in which we incorporated charge dependence in our shell-model calculation. First, the single-particle energies of the proton orbits were shifted relative to those of the neutrons. The amount of shift was determined from the spectrum of single-particle states in the closed-shell-plus-proton versus the closed-shell-plus-neutron nucleus, where the closed shell was taken to be the nucleus used as a closed-shell core in the shell-model calculation. We took these single-particle shifts from experiment and did not adjust them.

Second, we added a two-body Coulomb interaction among the valence protons and adjusted its strength so that the measured b -coefficient of the isobaric multiplet mass equation (IMME) was exactly reproduced. Third, we introduced a charge-dependent nuclear interaction by increasing all the $T = 1$ proton-neutron matrix elements by about 2% relative to the neutron-neutron matrix elements. The precise amount of this increment was determined by requiring agreement with the measured c -coefficient of the IMME. This strategy of constraining

TABLE III: Shell-model calculations of the isospin-mixing correction, δ_{C1} .

Parent nucleus	Measured		2002	This work				
	IMME coefficients [33]		$\delta_{C1}(\%)$	$E_x(0^+)$	$E_x(0^+)$	$\delta_{C1}(\%)$	$\delta_{C1}(\%)$	$\delta_{C1}(\%)$
	b (keV)	c (keV)	Ref. [4]	expt	SM	unscaled	scaled	
$T_z = -1$:								
^{10}C	-1.546	0.362	0.010(10)	6.18	9.24	0.005	0.011	0.010(10)
^{14}O	-2.493	0.337	0.050(20)	6.59	6.64	0.049	0.050	0.055(20)
^{18}Ne	-3.045(1)	0.347(1)	0.230(30)	3.71	4.07	0.116	0.140	0.155(30)
^{22}Mg	-3.814(1)	0.315(1)	0.010(10)	6.24	6.21	0.010	0.010	0.010(10)
^{26}Si	-4.535(2)	0.302(2)	0.040(10)	3.59	3.86	0.022	0.026	0.030(10)
^{30}S	-5.185(2)	0.275(2)	0.195(30)	3.79	3.80	0.137	0.138	0.155(20)
^{34}Ar	-5.777(2)	0.286(2)	0.030(10)	3.92	3.97	0.023	0.023	0.030(10)
^{38}Ca	-6.328(3)	0.284(3)	0.020(10)	3.38	3.21	0.026	0.023	0.020(10)
^{42}Ti	-6.712(3)	0.287(3)	0.220(100)	1.84	3.16	0.038	0.114	0.100(20)
$T_z = 0$:								
$^{26}\text{Al}^m$	-4.535(2)	0.302(2)	0.040(10)	3.59	3.86	0.025	0.028	0.030(10)
^{34}Cl	-5.777(2)	0.286(2)	0.105(20)	3.92	3.97	0.091	0.093	0.100(10)
$^{38}\text{K}^m$	-6.328(3)	0.284(3)	0.100(20)	3.38	3.21	0.099	0.089	0.105(20)
^{42}Sc	-6.712(3)	0.287(3)	0.060(30)	3.30 ^a	5.05	0.007	0.017	0.020(10)
^{46}V	-7.327(10)	0.276(11)	0.095(20)	3.57 ^a	4.86	0.040	0.075	0.075(30)
^{50}Mn	-7.892(30)	0.259(30)	0.055(20)	3.69	3.62	0.057	0.054	0.045(20)
^{54}Co	-8.519(25)	0.276(25)	0.040(15)	2.56	2.26	0.058	0.045	0.050(30)
^{62}Ga	-9.463(70)	0.265(25) ^b	0.330(40)	2.33	2.32	0.221	0.219	0.275(55)
^{66}As	-9.95(15)	0.262(25) ^b	0.250(40)	2.17 ^c	1.89	0.210	0.159	0.205(45)
^{70}Br	-10.48(23)	0.260(25) ^b	0.350(40)	2.01	2.05	0.332	0.346	0.350(40)
^{74}Rb	-10.82(25)	0.258(25) ^b	0.130(60)	0.508	0.523	0.122	0.129	0.130(60) ^d

^a Second excited 0^+ state; shell-model calculations indicate this state takes up most of the depletion from the analog state.

^b Estimated: extrapolated from a fit to c coefficients in 0^+ states in $A = 4n + 2$ nuclei, $10 \leq A \leq 58$; the data were taken from Ref. [33].

^c Estimated: value is the average of the excitation energy of the 0^+ states in ^{62}Zn and ^{70}Se .

^d No new calculations were performed for ^{74}Rb .

the charge-dependence in the effective interaction by requiring it to reproduce the coefficients of the IMME was adopted from the work of Ormand and Brown[31, 32].

Experimental data were used in one more way to constrain our calculations. If isospin were an exact symmetry, then the parent 0^+ ($T = 1$) state would decay exclusively to its analog state in the daughter nucleus. Beta transitions to all other 0^+ states in the daughter would be strictly forbidden. But, with isospin symmetry broken, weak transitions (with branching ratios measured in parts per million) can occur to these other 0^+ states. In this case, we write the Fermi matrix element squared to the n^{th} non-analog 0^+ state as

$$|M_F^n|^2 = 2\delta_{C1}^n \quad (19)$$

and the reduction in the analog transition Fermi matrix element squared as

$$|M_F|^2 = 2(1 - \delta_{C1}), \quad (20)$$

neglecting, in this context, the contribution of δ_{C2} . If all the 0^+ states of a given model space had the same $T = 1$

isospin designation, then the effect of isospin-symmetry breaking terms in the Hamiltonian would be to deplete the analog-transition strength by an amount that is exactly matched by the sum of the strengths to the non-analog states: *i.e.*

$$\delta_{C1} \simeq \sum_n \delta_{C1}^n. \quad (21)$$

In practice, with large shell-model calculations the 0^+ states in the model space will include some states whose isospin designation is not $T = 1$; and Eq. (21) is not then exactly correct. Nevertheless, it remains approximately true.

Significantly, in many cases the bulk of the analog state depletion shows up in a single excited 0^+ state, usually (but not always) the first excited one. This allows us once again to use experiment to constrain and refine our calculation. In the limit of only two-state mixing, perturbation theory would indicate that

$$\delta_{C1} \propto \frac{1}{(\Delta E)^2} \quad (22)$$

where ΔE is the energy separation of the analog and non-analog 0^+ states. Again, this is not an exact result, but it does highlight the importance of the shell-model Hamiltonian producing a good quality spectrum of 0^+ states with, in particular, the first excited non-analog 0^+ state calculated to have an excitation energy close to its experimental value¹. This is not always possible to achieve in the shell model, especially near closed shells where excited 0^+ states tend to exhibit strong deformations. We used two strategies to bring the calculation into line with experimental information. Our first was to adjust the centroids of the shell-model Hamiltonian matrix elements specifically to get the excited 0^+ state at about the right energy. Our second was to scale our calculated δ_{C1} value by a factor $(\Delta E)_{\text{theo}}^2/(\Delta E)_{\text{expt}}^2$, the ratio of the square of the excitation energy of the first excited 0^+ state in the model calculation to that known experimentally.

We list in Table III the experimental values [33] of the IMME coefficients, b and c , and the known excitation energy $E_x(0^+)$ of the first (or second) excited 0^+ state in the daughter nuclei. As explained, all our shell-model calculations were adjusted to reproduce exactly the values of b and c , and to match, as closely as possible the excitation energy of the excited 0^+ state. We compensated for any remaining discrepancies between the calculated and experimental values of $E_x(0^+)$ by scaling the results for δ_{C1} . As in Table II, we give (in columns 6–8) the results from *one sample calculation* for each nucleus. Then in column nine we present adopted δ_{C1} values that result from our assessment of the results of *all* calculations made for each decay, not just the ones shown in columns 6–8; the uncertainties were chosen to encompass the spread in the results from those calculations and to include the uncertainty in the IMME b and c coefficients. For comparison, in column 4 we list the values we adopted for δ_{C1} in 2002[4]. Our strategies have remained unchanged, but here we have additionally used some more recent shell-model effective interactions as listed in Sect. III A 3. In nearly all cases, the new values of δ_{C1} agree with the old values within their stated uncertainties.

For the heavier nuclei there are experimental data on Fermi transitions to the non-analog excited 0^+ states. The measured branching ratios [15, 34, 35, 36] have been converted to δ_{C1}^1 values, *via* Eq. (19), and listed in Table IV. Again, for each nucleus, we list just one representative calculation and our adopted value. The assigned error reflects both the spread among the different calculations and the uncertainties in the IMME coefficients. Our 2002 adopted values [4] are also listed. For nuclei $38 \leq A \leq 54$, with the possible exception of ^{50}Mn , the agreement between theory and experiment is entirely sat-

TABLE IV: Shell-model calculations of δ_{C1}^1 for Fermi decay to the first excited 0^+ state; see Eq. (19). The results are compared with experimental measurements where they are known. All values are expressed in %.

Parent	2002	This work			
nucleus	value[4]	unscaled	scaled	Adopted	expt
$T_z = 0$:					
$^{38}\text{K}^m$	0.090(30)	0.068	0.062	0.085(30)	$< 0.28^a$
^{42}Sc	0.020(20)	0.007	0.027	0.015(15)	$0.040(9)^b$
^{46}V	0.035(15)	0.008	0.024	0.025(20)	$0.053(5)^a$
^{50}Mn	0.045(20)	0.049	0.047	0.040(20)	$< 0.016^a$
^{54}Co	0.040(20)	0.049	0.038	0.050(20)	$0.035(5)^a$
^{62}Ga	0.085(20)	0.160	0.159	0.120(40)	$\leq 0.040(15)^c$
^{66}As	0.020(20)	0.110	0.087	0.050(30)	
^{70}Br	0.070(20)	0.226	0.235	0.150(80)	
^{74}Rb	0.050(30)	0.045	0.047	$0.050(30)^d$	$\leq 0.075^e$

^aFrom Hagberg *et al.* (1994) [34]

^bFrom Daehnick and Rosa (1985) [35] averaged with earlier results.

^cFrom Hyland *et al.* (2006) [15]

^dNo new calculations were performed for ^{74}Rb .

^eFrom Piechaczek *et al.* (2003) [36]

isfactory. But in the upper pf -shell, the calculated value for ^{62}Ga is three times larger than measured in recent experiments [15]. Shell-model calculations in this region are complicated by the massive size of the Hamiltonian matrices. To keep our calculations tractable, we kept the $f_{7/2}$ shell closed in these cases, but there is considerable evidence [29] that this could be a poor assumption.

IV. THE RADIATIVE CORRECTION

A. Prior to 1990

Conventionally, the radiative correction has been separated into two parts, one that contains the nucleus-dependent terms, called the ‘outer’ radiative correction, and one that is independent of the nucleus, the ‘inner’ radiative correction. Principally due to the work of Marciano and Sirlin (for example, Refs. [37, 38, 39]), the radiative correction applied to the uncorrected β -decay rate Γ_β^0 was expressed as follows:

$$\Gamma_\beta = \Gamma_\beta^0(1 + \delta'_R)(1 + \Delta_R^V) \quad (23)$$

$$\begin{aligned} \delta'_R &= \frac{\alpha}{2\pi} [\bar{g}(E_m) + \delta_2 + \delta_3] \xrightarrow{\text{large } E_m} \\ &\longrightarrow \frac{\alpha}{2\pi} \left[3 \ln \left(\frac{m_p}{2E_m} \right) + \frac{81}{10} - \frac{4\pi^2}{3} + \delta_2 + \delta_3 \right] \end{aligned} \quad (24)$$

¹ In a few cases, the state calculated to have the largest charge-dependent admixture was the second excited 0^+ state. In these cases we optimized the agreement between theory and experiment for the excitation energy of that state

$$\Delta_R^V = \frac{\alpha}{2\pi} \left[3 \ln \frac{m_W}{m_p} + \ln \frac{m_W}{m_A} + 2C - 4 \ln \frac{m_W}{m_Z} + \mathcal{A}_g \right] \quad (25)$$

$$= \frac{\alpha}{2\pi} \left[4 \ln \frac{m_Z}{m_p} + \ln \frac{m_p}{m_A} + 2C + \mathcal{A}_g \right], \quad (26)$$

where E_m is the maximum electron energy in β -decay, and m_W , m_p , m_Z are the masses of the W -boson, proton and Z -boson. The separation into outer and inner terms is accommodated in δ'_R and Δ_R^V respectively.

In the outer correction, δ'_R , the order- α term contains the function $\bar{g}(E_m)$: it is the average over the beta energy spectrum of the function $g(E, E_m)$, which was defined by Sirlin (see Eq. (20b) of Ref. [37]) and is not reproduced here. Its large- E_m limit is shown in Eq. (24), indicating that the expression is dominated by the logarithm, $\ln(m_p/(2E_m))$. The last two terms in the outer correction, δ_2 and δ_3 , represent corrections to order $Z\alpha^2$ and $Z^2\alpha^3$ respectively. The origin of the $\bar{g}(E_m)$ term – together with that of the leading term in the inner radiative correction, $3 \ln(m_W/m_p)$ – is the γW -box and bremsstrahlung diagrams, which are taken together to remove the divergence as the photon energy goes to zero. Both δ_2 and δ_3 also come from a standard QED calculation of the γW -box and bremsstrahlung graphs [40, 41], but in their case the electron was allowed to interact with the Coulomb field of the nucleus. Care was taken not to double count with the Fermi function. The calculation was complete to order $Z\alpha^2$ but only estimated in order $Z^2\alpha^3$.

In the inner correction, Δ_R^V , the second and third terms, $\ln(m_W/m_A) + 2C$, like the first term, also represent a γW box graph, but this time it involves an axial-vector weak interaction. The evaluation of this graph can be divided into two energy regimes: the high-energy (or short-distance) part given by the logarithm, and the low-energy (or long-distance) part denoted by $2C$. The parameter m_A , referred to as the low-energy cut-off, divides these two energy regimes. Marciano and Sirlin [38] allowed it to take on a range of values, $400 \text{ MeV} \leq m_A \leq 1600 \text{ MeV}$ (revised slightly by Sirlin [42] to be $m_{a_1}/2 \leq m_A \leq 2m_{a_1}$, with m_{a_1} being the A_1 -vector-meson mass). The low-energy component, $2C$, was approximated by its Born contribution

$$C \rightarrow C_{\text{Born}} = 3g_A(0.266)(\mu_p + \mu_n) = 0.885, \quad (27)$$

where $g_A = 1.26$ is the axial vector coupling constant accepted at the time and $(\mu_p + \mu_n) = 0.88$ is the nucleon isoscalar magnetic moment. The factor 0.266 is the value of the loop integral that was rendered finite by the use of dipole form factors for the nucleon electromagnetic, γN , and axial-vector, WN , vertices. The fourth term in Eq. (25), with the logarithm $\ln(m_W/m_Z)$, arises from ZW -box graphs; while the last term, \mathcal{A}_g , represents a small perturbative QCD correction that was evaluated by Marciano and Sirlin [39] to be $\mathcal{A}_g = -0.34$.

The value of the outer radiative correction as defined in Eq. (24), ranges from 1.39-1.65% for the known super-allowed emitters (see Ref. [4]). Following Sirlin [40], the assigned uncertainties are set equal to $(\alpha/2\pi)\delta_3$ as an estimate of the error made in stopping the calculation at that order. The value of the inner radiative correction as obtained from Eq. (26) with C from Eq. (27) is [39, 42]

$$\Delta_R^V(\text{old}) = 2.40(8)\%. \quad (28)$$

These results provide the essential foundation of the radiation corrections still used today. However a number of improvements have been introduced in the intervening 17 years.

B. A nuclear-structure dependent term

The low-energy part of the γW -box diagram for an axial-vector weak interaction, denoted $2C$, was approximated by its Born contribution in Eq. (27), and was evaluated on a single nucleon. However, in a finite nucleus with many nucleons present, Jaus and Rasche [43] observed that the two hadronic-interaction vertices, γN and WN , do not have to be with the same nucleon. Thus, in finite nuclei there can be two types of contributions: those in which γN and WN vertices are with the same nucleon and those in which they are not. The evaluation of the former terms yields expressions [44] that are proportional to τ_+ , the isospin ladder operator, and so are also proportional to the Fermi β -decay operator. Therefore, they produce a universal correction – the same in all nuclei – with the value C_{Born} , which is given in Eq. (27). The remaining terms, those in which the interactions are with different nucleons, must be evaluated with two-body operators that depend on the nuclear structure of the states involved. Thus, the expression for C given in Eq. (27) must be replaced by the following equation:

$$C = C_{\text{Born}} + C_{NS}, \quad (29)$$

where C_{NS} comprises the nuclear-structure dependent terms. Calculations of C_{NS} were first made in 1992 [44, 45].

A further modification was introduced in 1994 [46]. In calculations of C_{Born} that had been made up to that time, the axial-vector and electromagnetic coupling constants, g_A and $(\mu_p + \mu_n)$ – see Eq. (27) – had been given their free-nucleon values. Yet there is ample evidence in nuclear physics that coupling constants for spin-flip processes are quenched in the nuclear medium, with the amount of quenching varying from nucleus to nucleus. Thus, one should really be replacing $C_{\text{Born}}^{\text{free}}$, the value obtained with free-nucleon coupling constants, with $C_{\text{Born}}^{\text{quenched}}$. However, to separate the nucleus-dependent and nucleus-independent parts of the latter, we write

$$\begin{aligned} C_{\text{Born}}^{\text{quenched}} &= q C_{\text{Born}}^{\text{free}} \\ &= C_{\text{Born}}^{\text{free}} + (q - 1) C_{\text{Born}}^{\text{free}} \end{aligned} \quad (30)$$

where q is the factor by which the product of the weak and electromagnetic coupling constants is reduced in the medium relative to its free-nucleon value.

The first term in Eq. (30), which remains universal, is retained in the inner radiative correction, replacing C in Eq. (25). The second term becomes part of a separate nuclear-structure-dependent radiative correction, δ_{NS} , which also includes C_{NS}^{quenched} , the value of C_{NS} recalculated with quenched operators. This correction is written as

$$\delta_{NS} = \frac{\alpha}{\pi} \left[C_{NS}^{\text{quenched}} + (q-1)C_{\text{Born}}^{\text{free}} \right], \quad (31)$$

and is incorporated with the other nuclear-structure-dependent correction term, δ_C – see Eq. (5). Calculated values of δ_{NS} [4] range from -0.360% to +0.030%, each generally being smaller in magnitude than the corresponding value of δ_C .

We return to δ_{NS} in Sect. IV E.

C. Improvements to Δ_R^V

In 2005, Czarnecki, Marciano and Sirlin [47] revisited the $\mathcal{O}(\alpha^2)$ correction for neutron beta decay. They began by trivially updating the value of $C_{\text{Born}}^{\text{free}}$ to reflect the current value of the axial-vector coupling constant, $g_A = 1.27$, to get

$$C_{\text{Born}}^{\text{free}} = 0.891, \quad (32)$$

which replaces the value given in Eq. (27).

They then went on to re-evaluate Δ_R^V , focusing particularly on the leading log corrections. Using an established renormalization group summation [39] for the leading short-distance logs, $S(m_p, m_Z)$, they extended the method to the lower energy region between $2E_m$ and m_p to obtain $L(2E_m, m_p)$. This resulted in the replacements

$$1 + \frac{2\alpha}{\pi} \ln \frac{m_Z}{m_p} \rightarrow S(m_p, m_Z) = 1.02248 \quad (33)$$

$$1 + \frac{3\alpha}{2\pi} \ln \frac{m_p}{2E_m} \rightarrow L(2E_m, m_p), \quad (34)$$

where

$$L(2E_m, m_p) = 1.026725 \left[1 - \frac{2\alpha(m_e)}{3\pi} \ln \frac{2E_m}{m_e} \right]^{9/4}. \quad (35)$$

The complete radiative correction, RC, including order $Z\alpha^2$ and $Z^2\alpha^3$ terms, could then be written [47]

$$\begin{aligned} 1 + RC = & \left\{ 1 + \frac{\alpha}{2\pi} \left[\bar{g}(E_m) - 3 \ln \frac{m_p}{2E_m} \right] \right\} \\ & \times \left\{ L(2E_m, m_p) + \frac{\alpha}{2\pi} [2C_{\text{Born}}^{\text{free}} + \delta_2 + \delta_3] \right\} \\ & \times \left\{ S(m_p, m_Z) + \frac{\alpha(m_p)}{2\pi} \left[\ln \frac{m_p}{m_A} + \mathcal{A}_g \right] + NLL \right\}, \end{aligned} \quad (36)$$

where NLL is a next-to-leading log correction that Czarnecki *et al.* estimate to be $NLL = -0.0001$. The coefficient $\alpha(m)$ is a running QED coupling constant whose value at $m = m_p$ is $1/133.986$ and at $m = m_e$ is $1/137.089$ [47].

This new result can still be organized to preserve the separation of nucleus-dependent and nucleus-independent components. The separation we hereby adopt is

$$\begin{aligned} 1 + \delta'_R = & \left\{ 1 + \frac{\alpha}{2\pi} \left[\bar{g}(E_m) - 3 \ln \frac{m_p}{2E_m} \right] \right\} \\ & \times \left\{ L(2E_m, m_p) + \frac{\alpha}{2\pi} [\delta_2 + \delta_3] \right\} \end{aligned} \quad (37)$$

$$\begin{aligned} 1 + \Delta_R^V = & S(m_p, m_Z) + \frac{\alpha}{\pi} C_{\text{Born}}^{\text{free}} \\ & + \frac{\alpha(m_p)}{2\pi} \left[\ln \frac{m_p}{m_A} + \mathcal{A}_g \right] + NLL. \end{aligned} \quad (38)$$

We will use this separation here and in our future work on superallowed β decay. It results in a small change to the values of δ'_R and Δ_R^V that we used in our recent review [1].

D. Reduced uncertainty for Δ_R^V

In Sect. IV A we explained that the terms $\ln(m_w/m_A) + 2C$ in Eq. (25) arose from the γW -box graph for an axial-vector weak interaction. These two terms came from splitting the evaluation of this graph into two energy regimes. The division between the two regimes was chosen to be $m_A = 1.2$ GeV [42], roughly the mass of the A_1 resonance, and its range of uncertainty was taken to be from $m_A/2$ to $2m_A$. This *ad hoc* range determination actually produced the largest single contributor to the uncertainty in the CKM matrix element, V_{ud} .

To reduce the hadronic uncertainty in the radiative correction, Marciano and Sirlin [8] have looked again at the γW -box graph for an axial-vector weak interaction. This time they split it into three energy regimes, rather than two and, where possible, they drew on independent information to control their results:

- *Short distances*, $(1.5 \text{ GeV})^2 \leq Q^2 < \infty$: This is a domain where QCD corrections remain perturbative. Marciano and Sirlin added higher-order terms, noting that these terms are identical (in the chiral limit) to QCD corrections to the Bjorken sum rule for polarized electroproduction and can therefore be obtained from well-studied calculations for that process.
- *Intermediate distances*, $(0.823 \text{ GeV})^2 \leq Q^2 < (1.5 \text{ GeV})^2$: In this region, they used an interpolation function between low and high energies, motivated by vector-meson and axial-vector-meson

TABLE V: Calculated transition-dependent radiative correction, δ'_R , in percent units, and the component contributions. In our previous works (*eg.* Ref. [4]) δ'_R was defined as the sum of the contents of columns 2-4; this result is given in column 5 and labeled “Former δ'_R .” As explained in the text, we have now redefined δ'_R to include the additional term in column 6; the new values for δ'_R are given in the last column.

Parent nucleus	$\frac{\alpha}{2\pi}\bar{g}(E_m)$	$\frac{\alpha}{2\pi}\delta_2$	$\frac{\alpha}{2\pi}\delta_3$	Former δ'_R	$\frac{\alpha}{2\pi}\delta_{\alpha^2}$	Redefined δ'_R
$T_z = -1$:						
^{10}C	1.468	0.180	0.004	1.652	0.027	1.679(4)
^{14}O	1.286	0.226	0.008	1.520	0.023	1.543(8)
^{18}Ne	1.204	0.268	0.012	1.484	0.022	1.506(12)
^{22}Mg	1.122	0.307	0.017	1.446	0.020	1.466(17)
^{26}Si	1.055	0.342	0.023	1.420	0.019	1.439(23)
^{30}S	1.005	0.371	0.029	1.405	0.018	1.423(29)
^{34}Ar	0.963	0.396	0.035	1.395	0.017	1.412(35)
^{38}Ca	0.929	0.426	0.042	1.397	0.017	1.414(42)
^{42}Ti	0.906	0.456	0.050	1.412	0.016	1.428(50)
$T_z = 0$:						
$^{26}\text{Al}^m$	1.110	0.328	0.020	1.458	0.020	1.478(20)
^{34}Cl	1.002	0.390	0.032	1.425	0.018	1.443(32)
$^{38}\text{K}^m$	0.964	0.420	0.039	1.423	0.017	1.440(39)
^{42}Sc	0.939	0.451	0.047	1.436	0.017	1.453(47)
^{46}V	0.903	0.472	0.054	1.429	0.016	1.445(54)
^{50}Mn	0.873	0.494	0.062	1.430	0.015	1.445(62)
^{54}Co	0.844	0.513	0.071	1.428	0.015	1.443(71)
^{62}Ga	0.805	0.553	0.087	1.445	0.014	1.459(87)
^{66}As	0.791	0.570	0.095	1.456	0.014	1.470(95)
^{70}Br	0.776	0.591	0.105	1.473	0.013	1.49(11)
^{74}Rb	0.761	0.609	0.115	1.485	0.013	1.50(12)

dominance. By limiting the number of terms to three, they had sufficient matching conditions to determine the coefficients uniquely.

- *Long distances*, $0 \leq Q^2 \leq (0.823 \text{ GeV})^2$: Integrating the long-distance amplitudes up to $Q^2 = (0.823 \text{ GeV})^2$, where the integrand matches smoothly to the interpolation function, they obtained a smaller value for $C_{\text{Born}}^{\text{free}}$,

$$C_{\text{Born}}^{\text{free}} = 0.829, \quad (39)$$

than given in Eq. (32). However this smaller value is caused entirely by the reduction in the effective upper limit to the loop integration, and is almost completely compensated for by the consequently higher values obtained for the graph in the other energy regimes.

In the end, Marciano and Sirlin [8] find that the net effect of this re-evaluation of the γW -box axial graph is a very small reduction in the radiative correction of 1.4×10^{-4} . More important than this reduction, the new method provides a more systematic estimate of the

hadronic uncertainties. Allowing for a $\pm 10\%$ uncertainty for the $C_{\text{Born}}^{\text{free}}$ correction in Eq. (39), a $\pm 100\%$ uncertainty for the interpolator contribution in the intermediate region, and ± 0.0001 uncertainty from neglected higher order effects, Marciano and Sirlin [8] find the total uncertainty in the radiative correction is ± 0.00038 . This corresponds to more than a factor of two reduction in the loop uncertainty for hadronic effects (*cf.* Eq.(28)).

E. New values for δ'_R , Δ_R^V and δ_{NS}

We maintain the traditional separation of the radiative correction into a nucleus-dependent outer correction and a nucleus-independent inner correction – see Eqs. (37) and (38). This means that the outer correction, δ'_R , is slightly redefined and is now written as

$$\delta'_R = \frac{\alpha}{2\pi} [\bar{g}(E_m) + \delta_2 + \delta_3 + \delta_{\alpha^2}] \quad (40)$$

where the new term, δ_{α^2} , simply represents the difference between the definition of δ'_R given in Eq. (37) and that given in Eq. (24). It is the leading-log extrapolation of the logarithm $\ln(m_p/2E_m)$, which is contained in the function $\bar{g}(E_m)$. Values of δ_{α^2} and the redefined δ'_R are

TABLE VI: Calculated nuclear-structure-dependent radiative correction, δ_{NS} , in percent units, and the component contributions.

Parent nucleus	2002 $\delta_{NS}(\%)$	This work		
	Ref. [4]	C_{NS}^{quenched}	$(q-1)C_{\text{Born}}^{\text{free}}$	$\delta_{NS}(\%)$ adopted
$T_z = -1$:				
^{10}C	-0.360(35)	-1.318	-0.176	-0.345(35)
^{14}O	-0.250(50)	-0.844	-0.208	-0.245(50)
^{18}Ne	-0.290(35)	-1.051	-0.198	-0.290(35)
^{22}Mg	-0.240(20)	-0.750	-0.213	-0.225(20)
^{26}Si	-0.230(20)	-0.705	-0.227	-0.215(20)
^{30}S	-0.190(15)	-0.557	-0.242	-0.185(15)
^{34}Ar	-0.185(15)	-0.520	-0.257	-0.180(15)
^{38}Ca	-0.180(15)	-0.475	-0.271	-0.175(15)
^{42}Ti	-0.240(20)	-0.765	-0.241	-0.235(20)
$T_z = 0$:				
$^{26}\text{Al}^m$	0.009(20)	0.242	-0.227	0.005(20)
^{34}Cl	-0.085(15)	-0.118	-0.257	-0.085(15)
$^{38}\text{K}^m$	-0.100(15)	-0.158	-0.271	-0.100(15)
^{42}Sc	0.030(20)	0.391	-0.241	0.035(20)
^{46}V	-0.040(7)	0.093	-0.248	-0.035(10)
^{50}Mn	-0.042(7)	0.084	-0.254	-0.040(10)
^{54}Co	-0.029(7)	0.112	-0.261	-0.035(10)
^{62}Ga	-0.040(20)	0.087	-0.272	-0.045(20)
^{66}As	-0.050(20)	0.010	-0.278	-0.060(20)
^{70}Br	-0.060(20)	-0.085	-0.283	-0.085(25)
^{74}Rb	-0.065(20)	-0.026	-0.288	-0.075(30)

TABLE VII: Corrected $\mathcal{F}t$ values for the thirteen best known superallowed decays, obtained with the new correction terms presented in this work. The experimental ft values were taken from results in our 2005 survey [1] updated with more recent published data [6, 7, 9, 10, 11, 12, 13, 14, 15, 16]. The average $\mathcal{F}t$ value and the normalized χ^2 of the fit to a constant appears at the bottom.

Parent nucleus	$ft(s)$	$\delta'_R(\%)$	$\delta_{NS}(\%)$	$\delta_C(\%)$	$\mathcal{F}t(s)$
$T_z = -1$:					
^{10}C	3039.5(47)	1.679(4)	-0.345(35)	0.175(18)	3074.5(49)
^{14}O	3042.5(27)	1.543(8)	-0.245(50)	0.330(25)	3071.6(33)
^{22}Mg	3052.2(72)	1.466(17)	-0.225(20)	0.380(22)	3078.3(74)
^{34}Ar	3052.5(82)	1.412(35)	-0.180(15)	0.665(56)	3069.4(85)
$T_z = 0$:					
$^{26}\text{Al}^m$	3037.0(11)	1.478(20)	0.005(20)	0.310(18)	3072.5(15)
^{34}Cl	3050.0(11)	1.443(32)	-0.085(15)	0.650(46)	3071.3(21)
$^{38}\text{K}^m$	3051.1(10)	1.440(39)	-0.100(15)	0.655(59)	3071.7(24)
^{42}Sc	3046.4(14)	1.453(47)	0.035(20)	0.665(56)	3071.2(27)
^{46}V	3049.6(16)	1.445(54)	-0.035(10)	0.620(63)	3073.4(30)
^{50}Mn	3044.4(12)	1.445(62)	-0.040(10)	0.655(54)	3066.9(28)
^{54}Co	3047.6(15)	1.443(71)	-0.035(10)	0.770(67)	3066.7(33)
^{62}Ga	3075.5(14)	1.459(87)	-0.045(20)	1.48(21)	3073.0(72)
^{74}Rb	3084.3(80)	1.50(12)	-0.075(30)	1.63(31)	3077(13)
Average $\overline{\mathcal{F}t}$					3071.4(8)
χ^2/ν					0.6

given in Table V for all the superallowed transitions of interest.

The new inner correction is defined by Eq. (38), with $C_{\text{Born}}^{\text{free}}$ taken from Eq. (39). With its uncertainty obtained from Marciano and Sirlin [8], the result is

$$\Delta_R^V = (2.361 \pm 0.038)\%. \quad (41)$$

It is important to note that with the re-evaluation of $C_{\text{Born}}^{\text{free}}$, there is a consequent change in the nuclear-structure dependent correction δ_{NS} given in Eq. (31). Fortunately, the change is very small, being

$$(q-1)(C_{\text{Born}}^{\text{new}} - C_{\text{Born}}^{\text{old}})\left(\frac{\alpha}{\pi}\right) \simeq -0.3(-0.062)2.3 \times 10^{-3} \simeq 0.004\%. \quad (42)$$

In addition to making this change, we have also taken the opportunity to re-evaluate C_{NS} using the more recently available shell-model effective interactions described in Sect. III A 3. Our revised δ_{NS} values are listed in Table VI. As in Tables II and III, we give (in columns 3 and 4) the results from *one sample calculation* for each nucleus. Then in column 5 we present adopted δ_{NS} values that result from our assesment of *all* calculations made for each decay, not just the ones shown in columns 3 and 4; the uncertainties were chosen to encompass the spread in the results from those calculations. For comparison, in

column 2 we list the values we adopted for δ_{NS} in 2002 [4]. In all cases the new values agree with the old ones within the quoted uncertainties.

V. $\mathcal{F}t$ VALUES, V_{ud} AND CKM UNITARITY

We have calculated improved results for the correction terms δ_{C1} (see Table III), δ_{C2} (Table II) and δ_{NS} (Table VI); and, based on the work of Marciano and Sirlin, we have presented revised values for δ'_R (Table V) and Δ_R^V (Eq. (41)). We are now in a position to extract corrected $\mathcal{F}t$ values from the current world data for superallowed $0^+ \rightarrow 0^+$ transitions.

We use the same data set as that described in Sect. II: it represents an interim update of our 2005 complete survey [1] and includes ten additional published measurements [6, 7, 9, 10, 11, 12, 13, 14, 15, 16]. Results are given in Table VII for the thirteen superallowed transitions whose ft values are known to a precision of 0.3% or better. The $\mathcal{F}t$ values given in column 6 were obtained from the data in the preceeding columns through the application of Eq. (5). The corrected $\mathcal{F}t$ values are also plotted in Figure 2.

It is clear from the normalized χ^2 given on the bottom line of the table that the statistical agreement among the $\mathcal{F}t$ values remains excellent. Furthermore, it is evident from the figure that ^{46}V no longer shows any deviation from the overall average as it did in Fig. 1. However, it is equally evident that instead the ^{50}Mn and ^{54}Co $\mathcal{F}t$ values are now low, and by amounts that are no less statistically significant than the amount by which the ^{46}V value was previously high.

Rather than being a negative result, however, this possible discrepancy offers us the opportunity to use the cases of ^{50}Mn and ^{54}Co as a valuable test of our improved calculations. The Q_{EC} value for each of them

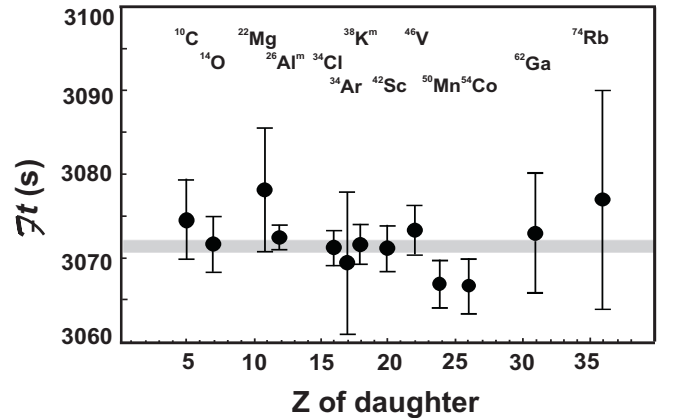


FIG. 2: Results for the new corrected $\mathcal{F}t$ values (from Table VII) for the thirteen best known superallowed decays. The corresponding uncorrected ft values appear in the left panel of Fig. 1. The shaded horizontal band gives one standard deviation around the average $\overline{\mathcal{F}t}$ value.

has been measured only twice with (claimed) high precision [48, 49], and one of these references [48] also included a measurement of the Q_{EC} value for ^{46}V , which Penning-trap measurements have recently shown [6, 11] to be low by 2 keV – more than three times its originally quoted standard deviation. If, as seems likely, the problem with the ^{46}V measurement in Ref. [48] is not limited to that measurement alone, then doubt is certainly cast on the ^{50}Mn and ^{54}Co Q_{EC} -value results quoted in that reference as well. New Penning-trap measurements of both Q_{EC} values are currently in progress [50], and the question should be settled shortly. If the Q_{EC} values in Ref. [48] prove to have been too low again, then the new Penning-trap measurements will serve to increase the $\mathcal{F}t$ values for ^{50}Mn and ^{54}Co and could well bring them into close agreement with the average $\overline{\mathcal{F}t}$ value. If so, this would add strong support to our new calculations.

The average corrected $\overline{\mathcal{F}t}$ value obtained from our new analysis, 3071.4(8) s, is lower by more than one standard deviation, compared to the comparable result obtained in our 2005 survey, 3072.7(8) s. If the new measurements do prove to increase the Q_{EC} values for ^{50}Mn and ^{54}Co , then this discrepancy will decrease slightly, but there is no avoiding the fact that the inclusion of some core orbitals in the nuclear-structure-dependent correction terms has increased the correction in a number of cases, which in turn leads to a reduction in their $\mathcal{F}t$ values. A significant change in the nuclear model has led to a significant change – but not a revolutionary one – in the average $\overline{\mathcal{F}t}$ value.

The new average $\overline{\mathcal{F}t}$ value yields a new value for V_{ud} via the equation

$$V_{ud}^2 = \frac{K}{2G_F^2(1 + \Delta_R^V)\overline{\mathcal{F}t}}, \quad (43)$$

where G_F is the well known weak-interaction constant for the purely leptonic muon decay [17]. It has been our practice when using the $\mathcal{F}t$ value in this context to add 0.85(85)s to its value to account for possible systematic errors in the treatment of the radial wave function in the calculation of δ_C . (This point is discussed in detail in section III C of Ref. [1].) Continuing this practice, we obtain the following result for the up-down element of the CKM matrix:

$$|V_{ud}| = 0.97418(26). \quad (44)$$

This result can be compared with the value 0.97380(40), which was obtained in 2005 [1]. The new value is (just) within the uncertainty of the previous value, and carries an uncertainty that is one third smaller.

The final step is to combine this new value of $|V_{ud}|$ with the other top-row elements of the CKM matrix, $|V_{us}|$ and $|V_{ub}|$, to test the unitarity of the matrix. Taking the values of the latter two elements from the 2006 Particle Data Group review [17] we obtain the stunning result

$$|V_{ud}|^2 + |V_{us}|^2 + |V_{ub}|^2 = 1.0000 \pm 0.0011. \quad (45)$$

Unitarity is fully satisfied with a precision of 0.1%.

VI. CONCLUSIONS

We have presented new calculations of the nuclear-structure-dependent corrections to superallowed $0^+ \rightarrow 0^+$ nuclear β decay. The calculations incorporate core orbitals in the shell model in cases where independent experimental information indicates that they are required. Where possible, they also make use of effective interactions that have been published since our previous calculation of these correction terms [4]. As in that work, we have included twenty transitions in our calculations, thirteen that are by now rather well measured and seven more that are likely to be accessible to precise measurements in the future.

The agreement among the corrected $\mathcal{F}t$ values for the thirteen well measured cases is very good, although there is a possible small discrepancy for the cases of ^{50}Mn and ^{54}Co . A new Penning-trap measurement of the Q_{EC} values for these two transitions is expected in the near future, and its effect on this discrepancy could serve to test the validity of our calculations.

With our new corrections, the value of $|V_{ud}|$ is increased by 0.04%, or by one standard deviation of the previous result [1]. With the new value, the sum of squares of the top-row elements of the CKM matrix is in perfect agreement with unitarity.

The improved calculations presented in this work were inspired by the remarkable recent improvements in experimental precision, particularly in the measurement of the ^{46}V Q_{EC} value. The only way that the calculated corrections can be tested and improved is by such precise measurements, both on the currently well-known transitions and on other as-yet-unstudied superallowed transitions that have larger calculated corrections. If the calculated correction terms replace the significant scatter in the measured ft values (see the left panel in Fig. 1) with a set of self-consistent corrected $\mathcal{F}t$ values, then they can surely be relied upon to produce a secure value for $|V_{ud}|$. The present calculations testify to the value of increased experimental precision.

Acknowledgments

The work of JCH was supported by the U. S. Dept. of Energy under Grant DE-FG03-93ER40773 and by the Robert A. Welch Foundation under Grant A-1397. IST would like to thank the Cyclotron Institute of Texas A & M University for its hospitality during annual two-month summer visits.

-
- [1] J.C. Hardy and I.S. Towner, Phys. Rev. C **71**, 055501 (2005).
- [2] J.C. Hardy and I.S. Towner, Phys. Rev. Lett. **94**, 092502 (2005).
- [3] J.C. Hardy, arXiv:hep-ph/0703165v1 (2007).
- [4] I.S. Towner and J.C. Hardy, Phys. Rev. C **66**, 035501 (2002).
- [5] W.E. Ormand and B.A. Brown, Phys. Rev. C **52**, 2455 (1995).
- [6] G. Savard, F. Buchinger, J.A. Clark, J.E. Crawford, S. Gulick, J.C. Hardy, A.A. Hecht, J.K.P. Lee, A.F. Levand, N.D. Scielzo, H.P. Sharma, K.S. Sharma, I. Tanihata, A.C. Villari, and Y. Wang, Phys. Rev. Lett. **95**, 102501 (2005).
- [7] T. Eronen, V. Elomaa, U. Hager, J. Hakala, A. Jokinen, A. Kankainen, I. Moore, H. Penttilä, S. Rahaman, J. Rissanen, A. Saastamoinen, T. Sonoda, J. Äystö, J.C. Hardy, and V.S. Kolhinen, Phys. Rev. Lett. **97**, 232501 (2006).
- [8] W.J. Marciano and A. Sirlin, Phys. Rev. Lett. **96**, 032002 (2006).
- [9] I.S. Towner and J.C. Hardy, Phys. Rev. C **72**, 055501 (2005).
- [10] B. Hyland, D. Melconian, G.C. Ball, J.R. Leslie, C.E. Svensson, P. Bricault, E. Cunningham, M. Domsbky, G.F. Grinyer, G. Hackman, K. Koopmans, F. Sarazin, M.A. Schumaker, H.C. Scraggs, M.B. Smith and P.M. Walker, J. Phys. G: Nucl. Part. Phys. **31**, S1885 (2005).
- [11] T. Eronen, V. Elomaa, U. Hager, J. Hakala, A. Jokinen, A. Kankainen, I. Moore, H. Penttilä, S. Rahaman, S. Rinta-Antilla, A. Saastamoinen, T. Sonoda, J. Äystö, A. Bey, B. Blank, G. Canchel, C. Dossat, J. Giovinazzo, I. Matea, N. Adimi, Phys. Lett. B **636**, 191 (2006).
- [12] G. Bollen, D. Davies, M. Facina, J. Huikari, E. Kwan, P.A. Lofy, D.J. Morrissey, A. Prinke, R. Ringle, J. Savory, P. Schury, S. Schwarz, C. Sumithrarachchi, T. Sun, L. Weissman, Phys. Rev. Lett. **96**, 152501 (2006).
- [13] P.H. Barker and A.P. Byrne, Phys. Rev. **73**, 064306 (2006).
- [14] V.E. Jacob, J.C. Hardy, J. Brinkley, C.A. Gagliardi, E. Mayes, N. Nica, G. Tabacaru, L. Trache, R.E. Tribble, Phys. Rev. Lett. **74**, 05502 (2006).
- [15] B. Hyland, C.E. Svensson, G.C. Ball, J.R. Leslie, T. Achtzehn, D. Albers, C. Andreoiu, P. Bricault, R. Churchman, D. Cross, M. Domsbky, P. Finlay, P.E. Garrett, C. Geppert, G.F. Grinyer, G. Hackman, V. Hanemaayer, J. Lassen, J.P. Lavoie, D. Melconian, A.C. Morton, C.J. Pearson, M.R. Pearson, A.A. Phillips, M.A. Schumaker, M.B. Smith, I.S. Towner, J.J. Valiente-Dobón, K. Wendt, and E.F. Zganjar, Phys. Rev. Lett. **97**, 102501 (2006).
- [16] J.T. Burke, P.A. Vetter, S.J. Freedman, B.K. Fujikawa and W.T. Winter Phys. Rev. C **74**, 025501 (2006).
- [17] W.-M. Yao *et al.*, Journal of Physics G **33**, 1 (2006).
- [18] D.D. Borlin, thesis, Washington University (1967), recorded in the nuclear data sheets of the National Nuclear Data Center: www.nndc.bnl.gov.
- [19] J.B. French and M.H. Macfarlane, Nucl. Phys. **26**, 168 (1961).
- [20] I.S. Towner, J.C. Hardy, and M. Harvey, Nucl. Phys. **A284**, 269 (1977).
- [21] S. Cohen and D. Kurath, Nucl. Phys. **73**, 1 (1965).
- [22] E.K. Warburton and B.A. Brown, Phys. Rev. C **46**, 923 (1992).
- [23] B.H. Wildenthal, in *Progress in Particle and Nuclear Physics*, edited by D.H. Wilkinson (Pergamon Press, Oxford 1984) Vol. **11**, p. 5.
- [24] B.A. Brown and W.A. Richter, Phys. Rev. C **74**, 034315 (2006).
- [25] T.T.S. Kuo and G.E. Brown, Nucl. Phys. **85**, 40 (1966).
- [26] A. Poves and A.P. Zuker, Phys. Reports **70**, 235 (1981).
- [27] W.A. Richter, M.G. van der Merwe, R.E. Julies and B.A. Brown, Nucl. Phys. **A523**, 325 (1991).
- [28] M. Honma, T. Otsuka, B.A. Brown and T. Mizusaki, Phys. Rev. C **65**, 061301(R) (2002).
- [29] M. Honma, T. Otsuka, B.A. Brown and T. Mizusaki, Phys. Rev. C **69**, 034335 (2004).
- [30] D.J. Millener and D. Kurath, Nucl. Phys. **A255**, 315 (1975).
- [31] W.E. Ormand and B.A. Brown, Nucl. Phys. **A440**, 274 (1985).
- [32] W.E. Ormand and B.A. Brown, Phys. Rev. Lett. **62**, 866 (1989).
- [33] J. Britz, A. Pape and M.S. Antony, Atomic Data and Nucl. Data Tables **69**, 125 (1998).
- [34] E. Hagberg, V.T. Koslowsky, J.C. Hardy, I.S. Towner, J.G. Hykawy, G. Savard and T. Shinozuka, Phys. Rev. Lett. **73**, 396 (1994).
- [35] W.W. Daehnick and R.D. Rosa, Phys. Rev. C **5**, 1499 (1985).
- [36] A. Piechaczek, E.F. Zganjar, G.C. Ball, P. Bricault, J.M. D'Auria, J.C. Hardy, D.F. Hodgson, V. Iacob, P. Klages, W.D. Kulp, J.R. Leslie, M. Lipoglavsek, J.A. Macdonald, H.-B. Mak, D.M. Moltz, G. Savard, J. von Schwarzenberg, C.E. Svensson, I.S. Towner, and J.L. Wood, Phys. Rev. C **67**, 051305(R) (2003).
- [37] A. Sirlin, Phys. Rev. **164**, 1767 (1967).
- [38] W.J. Marciano and A. Sirlin, Phys. Rev. D **29**, 75 (1984).
- [39] W.J. Marciano and A. Sirlin, Phys. Rev. Lett. **56**, 22 (1986).
- [40] A. Sirlin, Phys. Rev. **D35**, 3423 (1987); A. Sirlin and R. Zucchini, Phys. Rev. Lett. **57**, 1994 (1986).
- [41] W. Jaus and G. Rasche, Phys. Rev. **D35**, 3420 (1987).
- [42] A. Sirlin, in *Precision Tests of the Standard Electroweak Model*, edited by P. Langacker (World-Scientific, Singapore, 1994).
- [43] W. Jaus and G. Rasche, Phys. Rev. **D41**, 166 (1990).
- [44] I.S. Towner, Nucl. Phys. **A540**, 478 (1992).
- [45] F.C. Barker, B.A. Brown, W. Jaus and G. Rasche, Nucl. Phys. **A540**, 501 (1992).
- [46] I.S. Towner, Phys. Lett. **B333**, 13 (1994).
- [47] A. Czarnecki, W.J. Marciano and A. Sirlin, Phys. Rev. D **70**, 093006 (2005).
- [48] H. Vonach, P. Glaessel, E. Huenges, P. Maier-Komor, H. Roesler, H.J. Scheerer, H. Paul and D. Semrad, Nucl. Phys. **A278**, 189 (1977).
- [49] V.T. Koslowsky, J.C. Hardy, E. Hagberg, R.E. Azuma, G.C. Ball, E.T.H. Clifford, W.G. Davies, H. Schmeing, U.J. Schrewe and K.S. Sharma, Nucl. Phys. **A472**, 419 (1987).
- [50] T. Eronen *et al.*, private communication.